

Analysis of metastable regimes in a parallel channel single phase natural circulation system with RELAP5/MOD3.2

M.R. Gartia, D.S. Pilkhwal, P.K. Vijayan*, D. Saha

Reactor Engineering Division, Bhabha Atomic Research Centre, Trombay, Mumbai-400 085, India

Received 11 November 2005; received in revised form 6 November 2006; accepted 6 November 2006

Abstract

The objective of the present study is to assess the capability of RELAP5/MOD3.2 computer code to predict the metastable regime (multiple steady states) in a parallel channel system under natural circulation. To examine the basic behavior of such a system, an analysis was carried out for natural circulation flows in vertical multiple channel systems with non-uniform heat inputs. A three parallel channel configuration connected to common inlet and outlet headers with a down-comer, was investigated using RELAP5/MOD3.2 computer code. The results showed the existence of a metastable regime. It was seen that there are two steady state points for the same heat flux ratio differing in flow direction. Further the power level at which flow reversal occurs had been investigated. It was found that, if the power is increased in the down-flowing channel keeping the power of the other two channels constant, then it will start flowing up-wards only after reaching a critical value of power. Similarly, if the power of an up-flowing channel is decreased, it will start flowing down only after reaching another critical value of power. It was observed that the two critical values of power are not the same. It was found that the flow reversal power level depends upon the operating procedure, that is, rate of power rise or power set back. A non-dimensional heat flux ratio (N_H) has been defined to predict the flow reversal in parallel channel system. The reason for flow reversal has also been investigated. It was observed that the flow directions in the natural circulation loop follow the maximum density (averaged) difference among the channels.

© 2006 Elsevier Masson SAS. All rights reserved.

Keywords: Metastable regime; Parallel channel systems; Flow reversal

1. Introduction

Natural circulation flows in multiple-channel systems operating with various levels of heat inputs occur in diverse applications. One of these can be found in nuclear reactors where under certain normal operating or upset conditions, natural circulation flow cools the core. Unequally heated parallel channel systems can exhibit interesting flow behaviors during natural circulation. There may exist a metastable regime in parallel channel system with non-uniform heat flux. By definition, a system is in a state of metastable equilibrium if it is stable to small disturbances but not to large disturbances. Flow instabilities are undesirable in two-phase flow processes for several reasons. Flow oscillations can affect the local heat transfer characteris-

tics, possibly resulting in oscillatory wall temperature, or may induce boiling crisis (critical heat flux, departure from nucleate boiling, burnout, dryout). Hence it is of particular importance to predict the metastable regime and the threshold of flow instability, so that this can be taken care of in the design. Chato [1] studied, analytically and experimentally, the metastable regime in a three channel system with one channel heated, one channel unheated, and the third channel either heated or cooled. For this arrangement he found that two different stable flow rates can occur for a given set of channel heating rates. He has predicted the flow reversal of a heated channel from down-flow to up-flow while increasing power of the down-flowing channel, keeping the power of the heated upward flowing channel constant. But the range of power level at which metastable regime occurs has not been clearly shown. Zvirin [2] has theoretically studied the stability of various steady state flows in a thermosyphon with multiple vertical channels. He has found

* Corresponding author. Tel.: +91 22 25595157; fax: +91 22 25505151.
E-mail address: vijayanp@barc.gov.in (P.K. Vijayan).

Nomenclature

A	flow area	m^2	z	elevation	m
Ch	Channel		<i>Greek symbols</i>		
D	hydraulic diameter	m	ρ	density	kg m^{-3}
f	Darcy–Weisbach friction factor		$\Delta\rho$	density difference	kg m^{-3}
g	gravitational acceleration	m s^{-2}	$\bar{\rho}$	average density	kg m^{-3}
h	enthalpy	J kg^{-1}	<i>Subscripts</i>		
K	local pressure loss coefficient		DC	down-comer	
L	length	m	h	heated channel	
N_m	non-dimensional mass flow rate, W_{un}/W_h		t	total	
N_H	non-dimensional heat flux ratio, q_{un}/q_h		un	unheated channel	
P	pressure	N m^{-2}	1, 2, 3	channel number	
q	heat flux	W m^{-2}			
W	mass flow rate	kg s^{-1}			

a modified Rayleigh number to describe the onset of flows and instabilities. Takeda et al. [3] numerically and experimentally studied a system of four vertical channels with different heat generation rate. They found that a one-dimensional modeling of the channels could predict the reversal of a heated channel from down-flow to up-flow, but not from up-flow to down-flow. Yahalom and Bein [4] have suggested a down-flow preference number, which says that a heated channel with the highest value of non-dimensional preference number will flow downward. Todreas and Kazimi [5] defined an up-flow preference number. This says that in a parallel channel system in which the heated channels are in down-flow, the channel with the highest up-flow preference number will reverse first from down-flow to up-flow. Preference numbers can only tell which channels are favorable to flow reversal, but the question that still remains is exactly at what power or heat flux ratio the flow in a heated channel will reverse from up-flow to down-flow and down-flow to up-flow. Does rate of increment or decrement of power affect the power level at which flow reverses? Therefore, an analysis has been carried out to predict the metastable regime in a natural circulation system with three parallel vertical channels connected between common inlet and outlet headers and a down-comer.

In the present work, it has been shown that flow reversal can occur even before power is switched off. Parallel unequally heated channels connected between an inlet and an outlet header with a common down-comer exhibit interesting steady state and stability behaviors. For example, the density difference between the down-comer and any channel leads to a buoyancy force favoring upward flow in the heated channel. On the other hand, the density difference between two unequally heated channels favors downward flow in the low power channel. Analysis by Linzer and Walter [6] shows that the flow reverses in an upward flowing channel if the power is reduced below a critical value. The critical value of the heat flux ratio at which the flow reversal takes place decreases with decrease in the heat flux of the upward flowing channel. According to Linzer and Walter this is a problem during hot start-up in natural circulation boilers. A comprehensive study of flow reversal is needed as flow reversal is possible during refueling and defu-

eling of a nuclear reactor. Reverse flowing channels can cause voids in the inlet header and down-comer that can lead to instability. In the present work, the possible reason for flow reversal has been investigated. It is found that in a parallel channel natural circulation system with such mutually competing driving forces, the actual flow direction is decided by the greater of the two buoyancy forces. The present analysis also showed, with reverse flowing channels considerably large power is required to revert back to upward flow while raising the power for a single-phase system with three channels.

In the present analysis, the possible existence of hysteresis in the natural circulation loop has been investigated. The results showed that multiple steady states differing in flow direction may occur for certain heat flux. The region bounded by this hysteresis is the metastable regime as discussed by Chato [1]. The analysis also showed that the hysteresis regime depends on the rate of reduction or increase of power emphasizing the importance of operating procedure to avoid flow reversal. The possibility of the existence of the metastable regime has been investigated with non-uniform heat inputs with RELAP5/MOD3.2 [7] computer code.

2. Description of the loop

The loop considered for analysis consists of three vertical channels having equal diameters (Inside diameter = 25.5 mm, Thickness = 2.7 mm) and equal lengths (5 m) along with common down-comer of same dimensions as that of the channels. These channels are connected to an inlet header (plenum), (Inside diameter = 250 mm, Thickness = 2.7 mm, Length = 964 mm) at the bottom and same size of an outlet header at the top. The channels are heated with equal power input from the outside and the down-comer is kept unheated. Equal amount of heat is assumed to be removed through a tube-in-tube cooler (Inside diameter = 150 mm, Thickness = 2.7 mm) at the top header. The structural material for the loop wall was SS-316 and the volumetric heat capacity of the material used in the analysis was $3.83 \times 10^6 \text{ J m}^{-3} \text{ K}^{-1}$. The wall roughness was considered to be equal to $45 \times 10^{-6} \text{ m}$. The working fluid was water. The schematic of the loop is shown in Fig. 1.

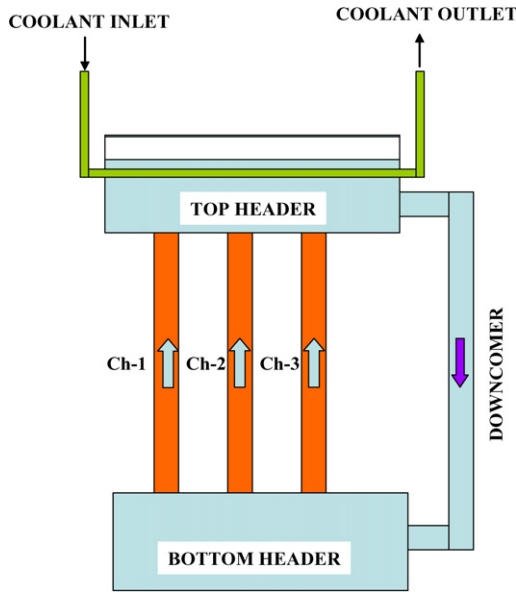


Fig. 1. Schematic of the natural circulation loop.

3. Modeling and nodalization scheme

The different components of the three parallel channel systems are modeled as pipes (control volumes) interconnected by junctions. The pipes are modeled as pipe volumes with corresponding cross-sectional flow area and lengths. The downcomer, top and bottom header are also modeled as pipe volumes. Our system is natural circulation based, which is driven by the density difference. The plenum is modeled as pipe, since the density distribution among its volumes can be accounted. Usually, the plena are modeled as branch components (which are a single volume) in the RELAP5/MOD3.2 nodalization scheme. Use of branch component will not give the variation of pressure in the plena. The three parallel channels are modeled with the help of appropriate heat structures. Thermal stratification is neglected in the present analysis. The nodalization scheme is shown in Fig. 2.

A grid independence test was performed by varying the number of grids from 5 to 100 for the heated section. It was found that the results are not significantly different after increasing the number of grids beyond 40. The result from the grid independence test is shown in Fig. 3. Hence 40 nodes were used for the heater section in the present analysis. The time step employed was 0.001 sec. The heat transfer from the primary (shell side) to secondary (tube side) of the cooler is modeled with an appropriate heat structure. The inlet and outlet of cooler were modeled by two time dependent volume (TDV) which will ensure the constant boundary conditions.

4. Initial conditions & cases studied

The initial conditions were corresponding to ambient pressure (1 bar) and temperature (300 K) with zero mass flow rates. The applicability of RELAP5/MOD3.2 has been well established for natural circulation systems under high tem-

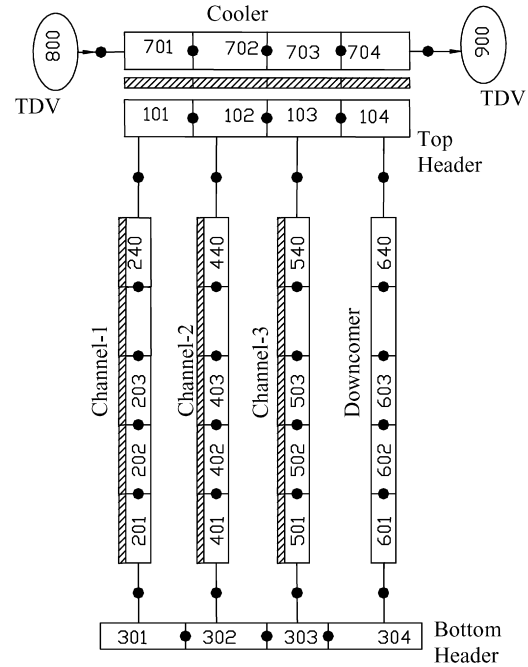


Fig. 2. Nodalization scheme for the natural circulation loop.

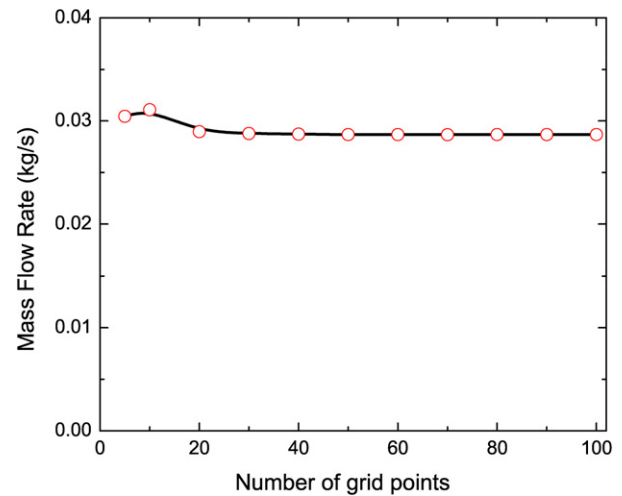


Fig. 3. Grid independence test.

perature and high pressure condition [8–10]. The validity of RELAP5/MOD3.2 computer code at atmospheric conditions was checked for the single-phase natural circulation flow by Kamble et al. [11] in a rectangular loop. They found that the steady state flow rate predictions by the RELAP5/MOD3.2 computer code are in good agreement with the experimental results.

Four cases were studied in the present analysis. Out of these, in two cases all the three channels have equal initial heat fluxes of either 10 kW m^{-2} or 5 kW m^{-2} . In the third case, the initial heat fluxes in two of the channels were 10 kW m^{-2} each and the third channel was unheated. In the fourth case the initial heat fluxes in two of the channels were 5 kW m^{-2} each and the third channel was kept unheated. In all the cases the steady state was achieved.

Table 1
Cases studied with initial heat fluxes (kW m^{-2})

Case No.	Ch-1	Ch-2	Ch-3
Initial heat flux			
1	10	10	10
2	5	5	5
3	10	0	10
4	5	0	5
Heat flux during transient conditions			
1	10	Decrease power till it reverses the flow	10
2	5	Decrease power till it reverses the flow	5
3	10	Increase power till it reverses the flow	10
4	5	Increase power till it reverses the flow	5

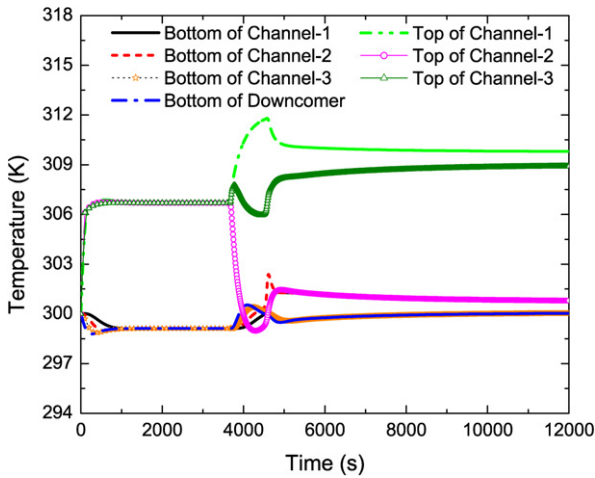


Fig. 4. Temperature variation in different channels (Case-1).

The transient study was carried out both by decreasing or increasing the heat flux. The details of the different cases studied are tabulated in Table 1.

5. Results and discussions

5.1. Transient for Case-1

In Case-1 the initial steady state has been achieved with equal heat flux of 10 kW m^{-2} to each of the three channels. The power is equal in all the heated channels. The transient was started long after steady state was achieved. During the transient in one of the channel (Ch-2) the heat flux was reduced from 10 kW m^{-2} with a particular rate of $10 \text{ W m}^{-2} \text{ s}^{-1}$. Fig. 4 shows the variation of temperatures at bottom and top of different channels. It is seen from this figure that the channel in which the heat flux is reduced, the temperature of the channel also reduces. As a result of decrease in temperature the density in the channel rises. The temperatures in the other two heated channels decrease because of the rise in the mass flow rate in these channels. Hence the densities in those two channels also rise slightly.

5.1.1. Explanation for flow reversal for Case-1

Fig. 5 shows the difference in densities at two ends of different channels. The variations of mass flow rate in the different

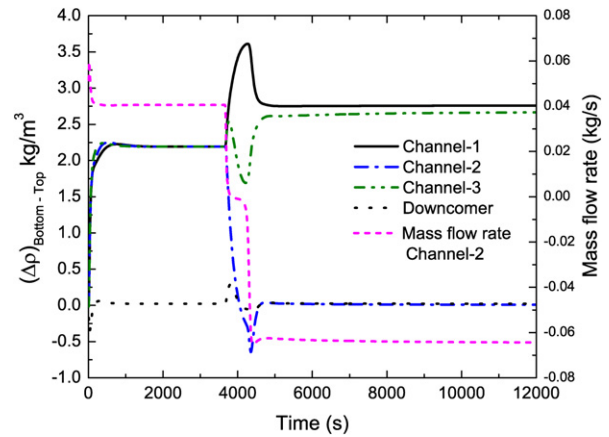


Fig. 5. Variation of difference in densities in different channels (Case-1).

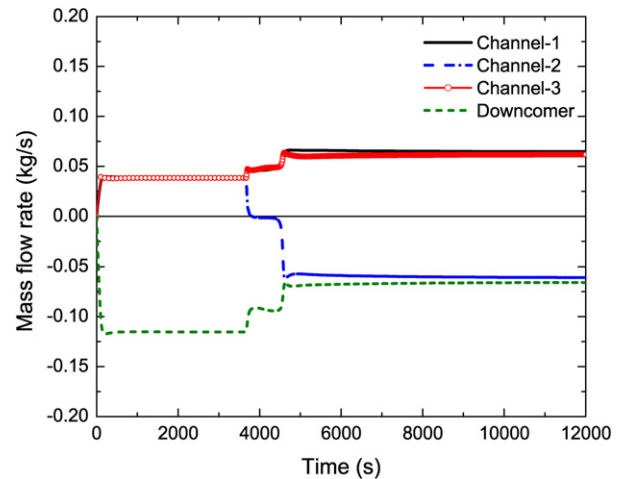


Fig. 6. Junction flow rate at the top header (Case-1).

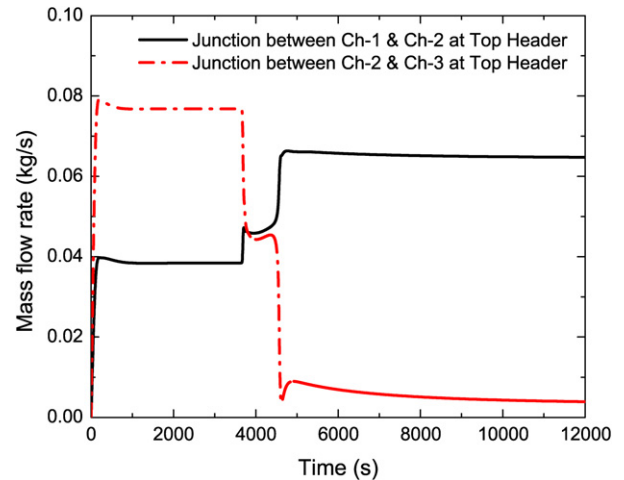


Fig. 7. Mass flow rate variations in different channels (Case-1).

channels are shown in Fig. 6. From these figures it is seen that, the flow reversal is taking place when the density difference is the minimum in Ch-2. Also the flow direction in Ch-2 will be decided by the channel with the maximum density difference. As a result, a local loop will be set up between Ch-1 and Ch-2. After flow reversal, as shown in Fig. 7, the flow rate at the junc-

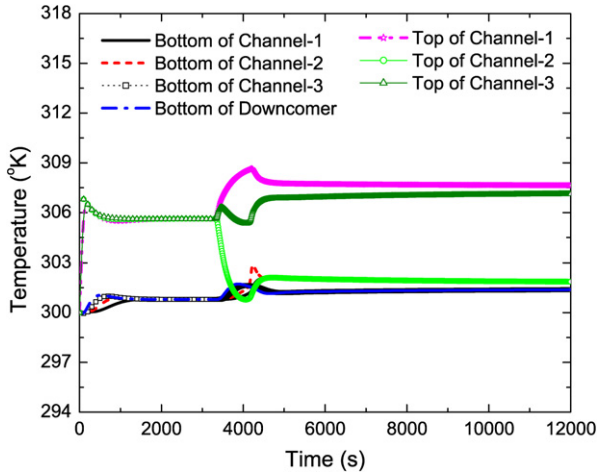


Fig. 8. Temperature variation in different channels (Case-2).

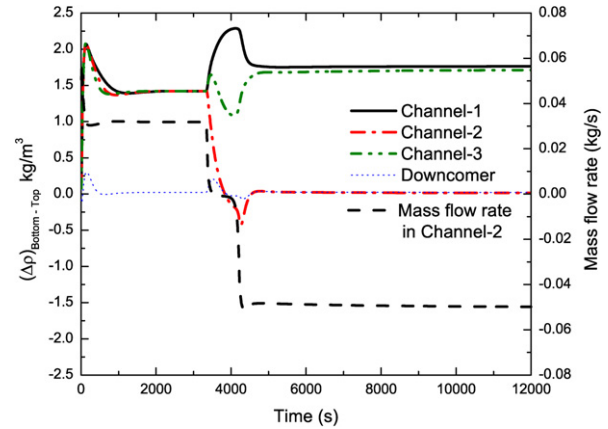


Fig. 10. Density difference between the bottom and top of different channels (Case-2).

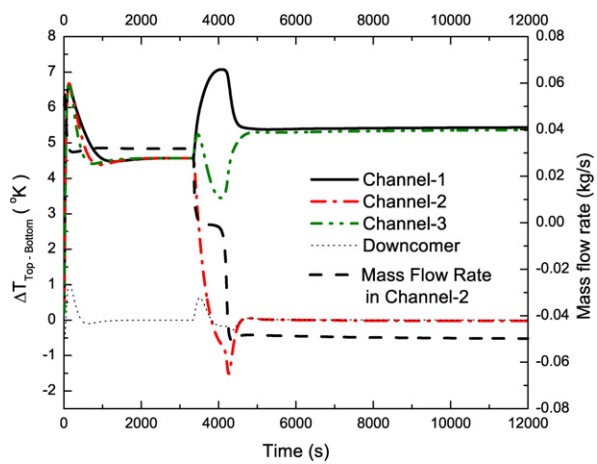


Fig. 9. Temperature difference between the top and bottom of different channels (Case-2).

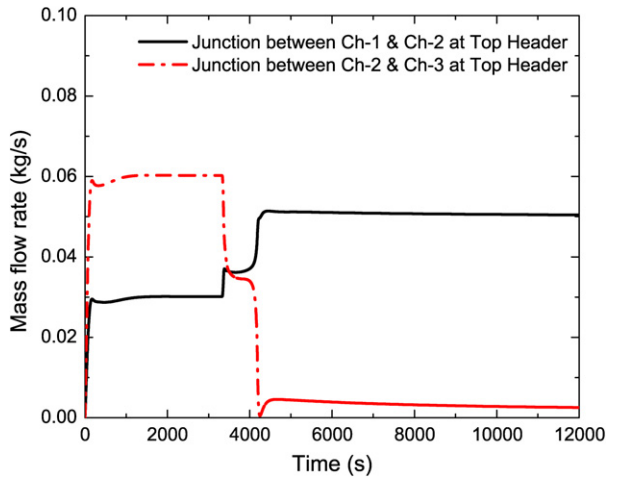


Fig. 11. Junction flow rate at the top header (Case-2).

tion between Ch-2 and Ch-3 drastically reduces to nearly zero value. This further confirms that a local loop has indeed been formed between Ch-1 and Ch-2. Since the flow direction in Ch-1 is upward, the flow direction for Ch-2 must be downward. The mass flow rate in the channel in which heat flux was decreased, falls gradually and after some time the flow reversal takes place. Consequently the flow rate in the other two channels increases. An analytical explanation for flow reversal has been given in Appendix A.

5.2. Transient for Case-2

In Case-2, the initial heat flux employed in each channel (Ch-1, Ch-2 & Ch-3) was 5 kW m^{-2} and steady state was achieved. The power in Ch-2 was decreased from 5 kW m^{-2} with a particular rate of $10 \text{ W m}^{-2} \text{ s}^{-1}$. The effect of decreasing the power on temperatures, difference in temperatures at two ends, difference in densities at two ends, junction flow rates and mass flow rates are shown in Figs. 8, 9, 10, 11 and 12 respectively. The nature of the curves is similar to those obtained in Case-1. Here also the flow reversal in Ch-2 was seen at time

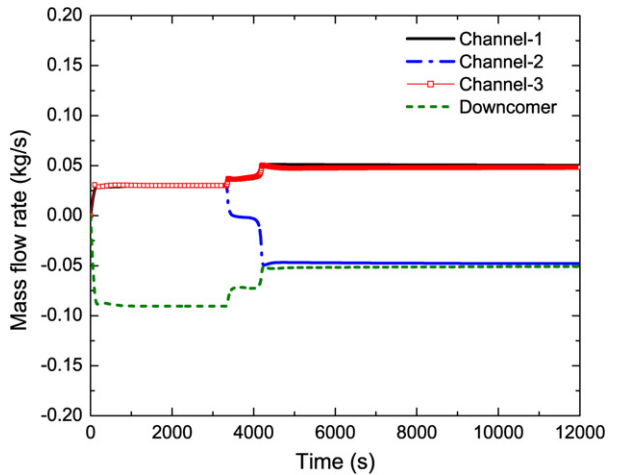


Fig. 12. Mass flow rate variations at different channels (Case-2).

when the difference in densities at the top and bottom end of Ch-2 is the minimum.

5.2.1. Explanation for flow reversal for Case-2

To explain the flow reversal phenomena, the average density difference among the channels was taken for analysis. The re-

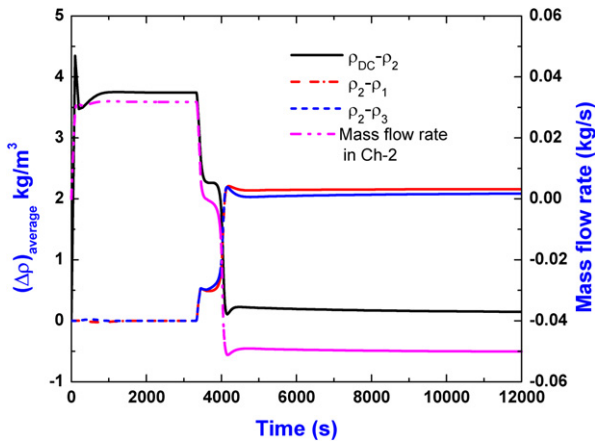


Fig. 13. Variation of average density difference among the channels (Case-2).

sult is shown in Fig. 13. This result corresponds to Case-2. As shown in Fig. 13, the reason for the flow reversal is the local loop set up between Ch-1 and Ch-2. It is evident from the fact that the difference in average densities between Ch-1 and Ch-2 is the maximum. Since, the local loop has been set up between Ch-1 and Ch-2, which is clear from Fig. 11 as there is no flow in the junction between Ch-2 and Ch-3. Also, as the flow in Ch-1 is in upward direction, the flow in the Ch-2 has to be in downward direction. Therefore, it is clear from Fig. 13 that density difference is the main driving force for flow reversal and channels with maximum density difference will decide the direction of flow.

5.3. Transient for Case-3

In Case-3 the initial steady state has been achieved with heat flux of 10 kW m^{-2} in two channels (Ch-1 and Ch-3) and Ch-2 remains unheated. The initial flow direction in heated channels was upward while in the unheated channel and down-comer, it was downward. The transient was initiated by heating the unheated channel (Ch-2). During transient the heat flux in the unheated channel was increased from 0 kW m^{-2} with a particular rate of $10 \text{ W m}^{-2} \text{ s}^{-1}$ up to a heat flux where the flow reversal takes place. The heating in this channel causes the coolant temperature to rise as shown in Fig. 14.

5.3.1. Explanation for flow reversal for Case-3

As the temperature in Ch-2 increases (because of heating), the density decreases. The change in density causes the flow to reduce in the downward direction and changes the direction slowly. The change in density difference in hot leg and cold leg causes the flow to reverse in this channel. Consequently the mass flow rate in the other two already heated channels decreases slightly. Due to the decrease in mass flow, the temperatures in the heated channels rise. Again because of the rise in temperature, the density in the channels decreases. The variation of density difference and mass flow rate is shown in Figs. 15 and 16 respectively.

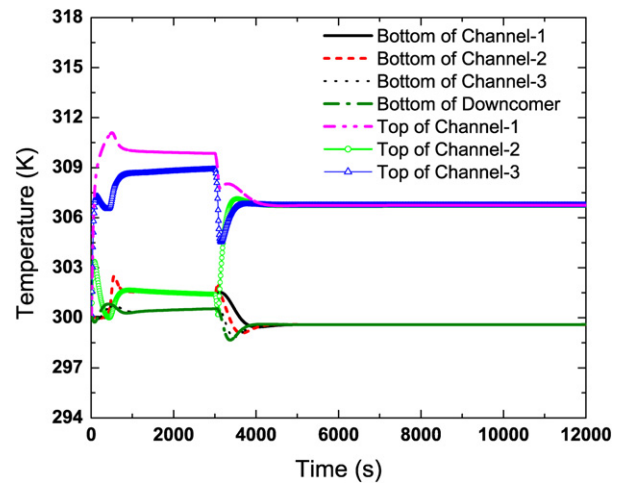


Fig. 14. Temperature variation at different channels (Case-3).

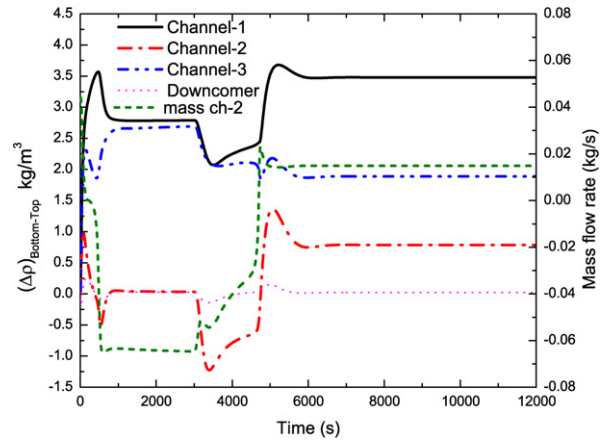


Fig. 15. Densities variation at different channels (Case-3).

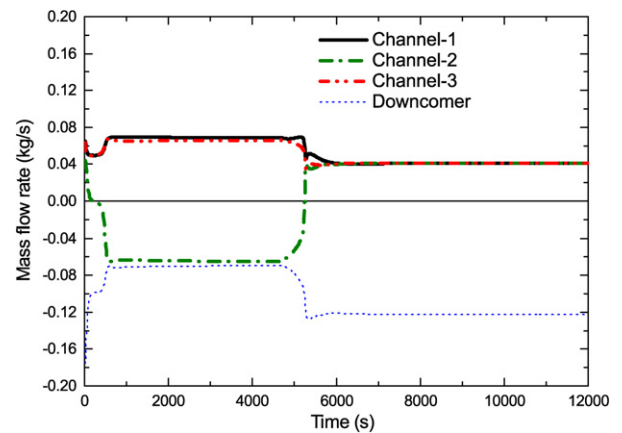


Fig. 16. Mass flow rate at different channels (Case-3).

5.4. Transient for Case-4

For the Case-4, two channels (Ch-1 and Ch-3) are at an equal heat flux of 5 kW m^{-2} each and Ch-2 was unheated. The flow direction in heated channels was upward before the transient was initiated while in the unheated channel and down-comer, it was downward. During transient the heat flux in the

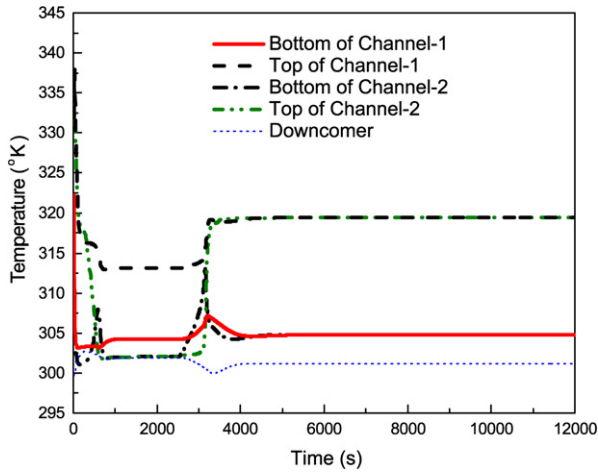


Fig. 17. Temperature variation at different channels (Case-4).

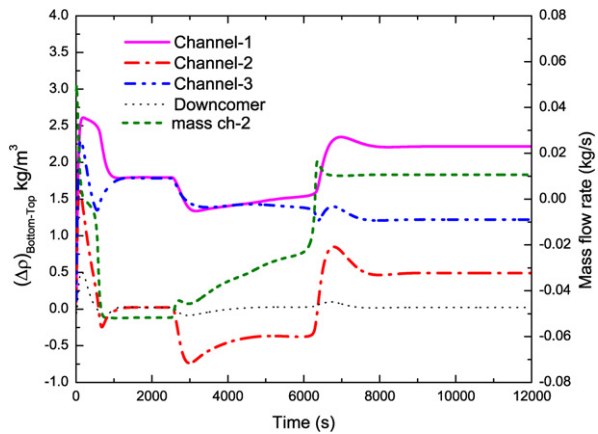


Fig. 18. Densities variation at different channels (Case-4).

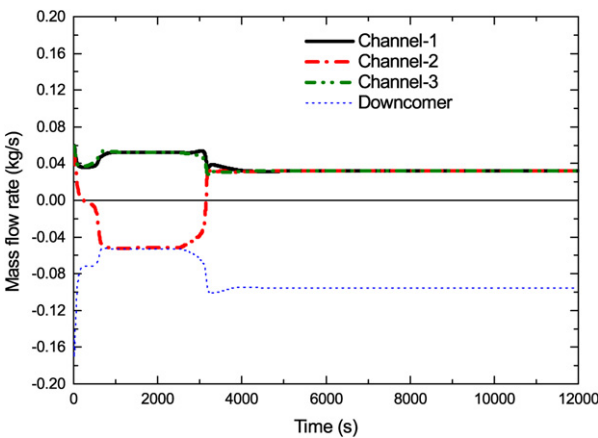


Fig. 19. Mass flow rate at different channels (Case-4).

unheated channel was increased from 0 kW m^{-2} with different rates up to a heat flux when flow reversal takes place. The effect of increasing the power in unheated channel on temperatures, densities and mass flow rates were found to be similar to that of Case-3 and are shown in Figs. 17, 18 and 19 respectively. These are shown for a particular heat flux increase rate of $10 \text{ W m}^{-2} \text{ s}^{-1}$.

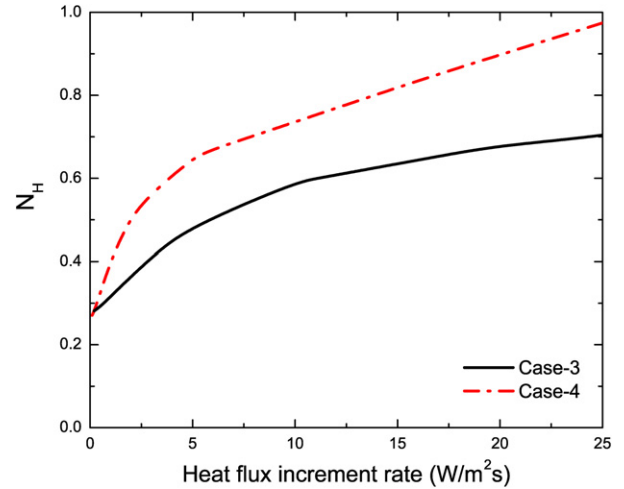


Fig. 20. Variation of N_H with heat flux increment rate.

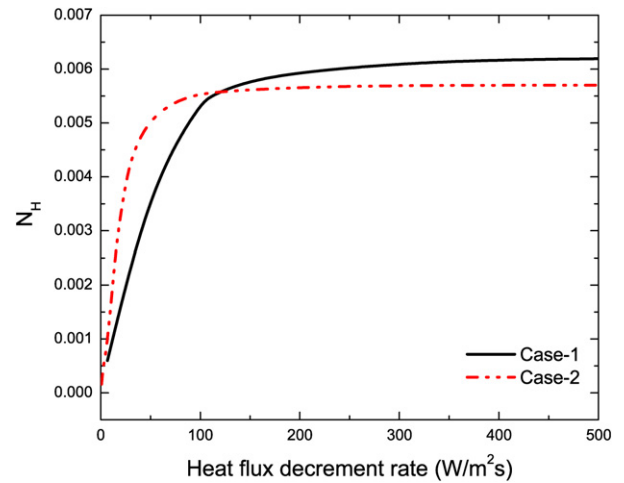


Fig. 21. Variation of N_H with heat flux decrement rate.

5.5. Effect of increment/ decrement rate on flow reversal power level

The analyses were repeated for different increasing and decreasing rates of power. Figs. 20 and 21 show variation of flow reversal heat flux ratio, $N_H (= q_{un}/q_h)$ with heat flux increment and decrement rate respectively. It is seen that N_H increases with the increase in heat flux increment rate. Also for the same heat flux increment rate, the ratio at which flow reversal occurs (N_H) is higher for lower initial heat flux (Case-4). On the other hand, as seen from Fig. 21, beyond heat flux decrement rate of $100 \text{ W m}^{-2} \text{ s}^{-1}$, for the same heat flux decrement rate, N_H is higher for higher initial heat flux (Case-1). Fig. 22 shows variation of heat fluxes at which flow reverses with heat flux increment/decrement rate for all the cases (Case-1 to Case-4).

5.6. Effect of initial heat flux on N_H

Fig. 23 shows the variation of non-dimensional mass flow rate, $N_m (= W_{un}/W_h)$ with non-dimensional heat flux ratio, N_H , for the Case-3 & Case-4. Initially the heat flux in the unheated channel is zero (i.e. $q_{un} = 0$). The flow in the unheated

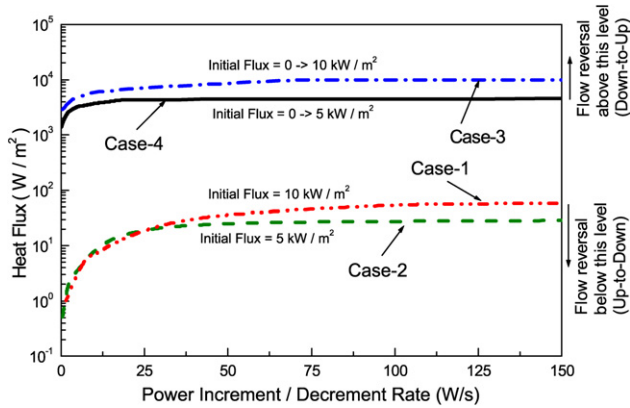


Fig. 22. Effect of initial heat flux and operating procedure on flow reversal heat flux level.

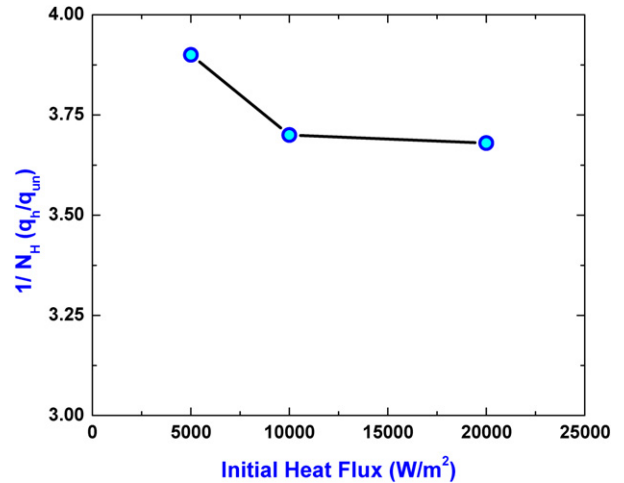


Fig. 24. Effect of initial heat flux values on $1/N_H$.

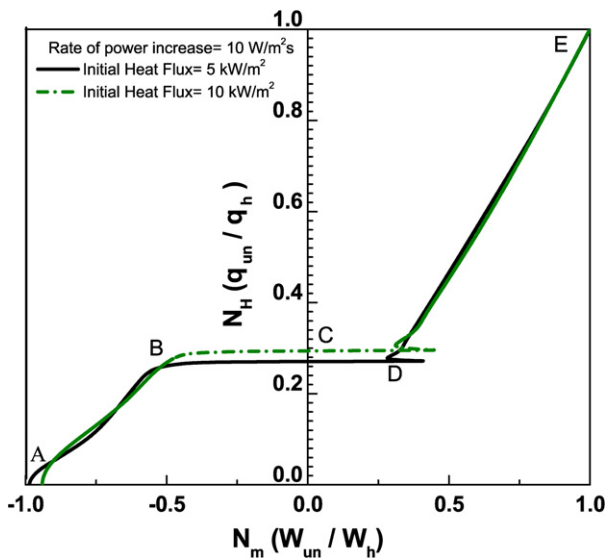


Fig. 23. Variation of non-dimensional heat flux ratio (N_H) at different initial heat fluxes (Case-3 & Case-4).

channel is downward while the flow in the heated channel is upward (i.e. initially when $N_H = 0$, N_m is a negative quantity). This state is shown at point A. As soon as we start heating in Ch-2, the flow in this channel decreases in downward direction with N_H . There is a critical value of N_H at which the flow reverses. This value is corresponding to point B. There is a jump in curve from B to D, through point C where N_m is zero. With further increase in N_H , the value of N_m increases. It should be noted that the above plot is for particular value of initial heat fluxes and for the case of power increase ($=10 \text{ W m}^{-2} \text{ s}^{-1}$). The curve will be different for different initial value of heat flux and different operating procedure (viz. power rise and power set back). Fig. 24 shows the variation of $(1/N_H)$ with three different initial heat flux values. It is seen that the ratio $(1/N_H)$ decreases with increase in initial heat flux. This is in contrast to the results obtained by Linzer and Walter [6] where this value was increasing with increase in initial heat flux value. This may be due to the difference in flow conditions, i.e. ours is a single-phase flow condition and in their case it was two-phase flow.

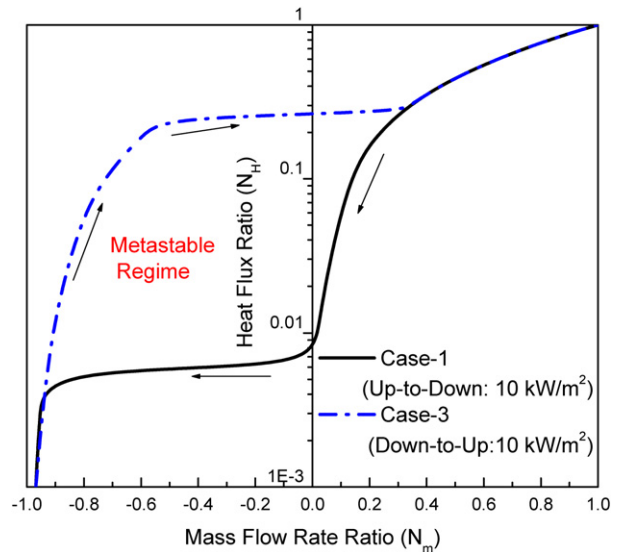
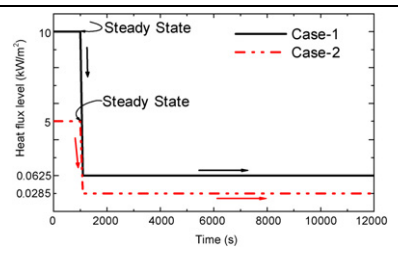
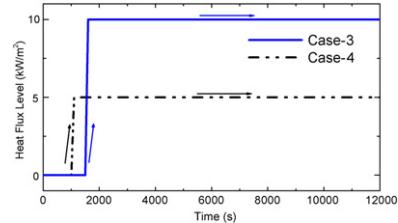
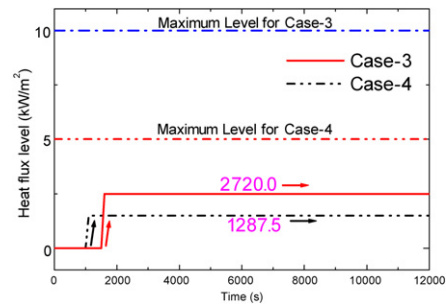


Fig. 25. Hysteresis effect of natural circulation loop at steady state.

5.7. Metastable regime (hysteresis effect of loop at steady state)

Fig. 25 shows both the power levels (power rise and power set-back) at which flow reversal occurs. It can be seen that in the case of power rise, the level at which flow reversal takes place is higher than that of power level corresponding to power set-back. There is a certain region bounded by a range of heat flux ratios where there are two different steady state points differing in flow direction corresponding to a single heat flux ratio. This special case of static instability is characterized by multiple steady states in different flow directions. The region bounded by this multiple steady state points is known as metastable regime. Welander [12] and Creveling et al. [13] analyzed a single channel system where they observed oscillatory behavior of flow before the reversal. In the experiments of Bau et al. [14], these phenomena were also observed. However, Yahalom and Bein [4] and Linzer and Walter [6] have not reported this type of oscillatory behavior before flow reversal in parallel channel system in conformity with the present findings.

Table 2
Non-dimensional heat flux ratio for different operating procedures and different initial heat fluxes

Case No.	Initial heat flux in Ch-2	Final heat flux in Ch-2	Rate [$W s^{-1}$]	N_H at flow reversal	Ratio (q_h/q_{un})	Operating procedure
1	10000	62.5	765	0.00625	160	
	10000	38.5	50	0.00385	259.64	
	10000	6.0	6.66	0.0006	1666.67	
2	5000	28.5	163	0.0057	735.4	
	5000	19.5	25	0.0039	256.4	
	5000	2.5	2.5	0.0005	2000.0	
3	0.0	8614.5	50	0.8615	1.16	
	0.0	5900.0	10	0.59	1.7	
	0.0	2815.0	0.1	0.28	3.6	
4	0.0	4872.5	25	0.97	1.026	
	0.0	3240	5	0.65	1.54	
	0.0	1353.4	0.1	0.27	3.7	
3	0.0	2720.0	2.72	0.272	3.67	
4	0.0	1287.5	1.29	0.26	3.88	

The typical values of the non-dimensional heat flux ratio (N_H) for different initial heat fluxes and operating procedures are shown in Table 2.

6. Conclusions

The possibility of the existence of a metastable regime in multiple channel systems with non-uniform heat inputs has been studied. To examine the basic behavior of such a system, a three parallel channel set up with a down-comer was investigated with RELAP5/MOD3.2 computer code. It was found that flow reversal can occur even before power is switched off. It is seen that corresponding to certain range of heat flux ratio there are two different steady state points differing in flow direction. It was found that, if the power is increased in the down-flowing channel keeping the power of the other two channels constant, then it will start flowing up-wards only after reaching a critical value of power. Similarly, if the power of an up-flowing channel is decreased, it will start flowing down only after reaching another critical value of power. It was observed that the corresponding two critical values of power are not the same. The region bounded by this two critical value (hysteresis region) has been termed as metastable regime.

It was found that in a parallel channel natural circulation system with mutually competing driving forces, the actual flow direction is decided by the greater of the two buoyancy forces.

The present analysis also showed, with reverse flowing channels considerably large power is required to revert back to upward flow while raising the power for a single-phase system with three channels. A non-dimensional heat flux ratio (N_H) has been proposed to predict the flow reversal. The present analysis also showed that the power level at which flow reversal takes place depends upon the initial starting power which will be useful in predicting a safe power level for a rational start-up procedure for nuclear reactors. The analysis also showed that the hysteresis regime depends on the rate of reduction or increase of power emphasizing the importance of operating procedure to avoid flow reversal.

Appendix A. Analytical derivation of flow reversal criteria

A.1. Governing equations

The one-dimensional steady state Navier–Stokes equations for single-phase natural circulation system can be written as follows:

Continuity equation:

$$\frac{d}{ds} \left(\frac{W}{A} \right) = 0 \quad (\text{A.1})$$

Energy equation:

$$\frac{W}{A} \frac{dh}{ds} = \begin{cases} \frac{4q_h}{D_h} & \text{heater} \\ 0 & \text{adiabatic pipes} \\ -\frac{4q_c}{D_c} & \text{cooler} \end{cases} \quad (\text{A.2})$$

Momentum equation:

$$\frac{W^2}{A^2} \frac{d}{ds} \left(\frac{1}{\rho} \right) = -\frac{dP}{ds} - \rho g \sin \theta - \frac{f W^2}{2D\rho A^2} - \frac{K W^2}{2\rho A^2 L_t} \quad (\text{A.3})$$

where θ is the angle with the horizontal in the direction of flow. The second term on the right-hand side of Eq. (A.3) represents the body force per unit volume whereas the third and fourth terms respectively represent the distributed and the local friction forces per unit volume. Noting that $v = 1/\rho$ and integrating the momentum equation around the circulation loop

$$\frac{W^2}{A^2} \oint dv = -\oint dP - g \oint \rho dz - \frac{f W^2 L_t}{2D\rho A^2} - \frac{K W^2}{2\rho A^2} \quad (\text{A.4})$$

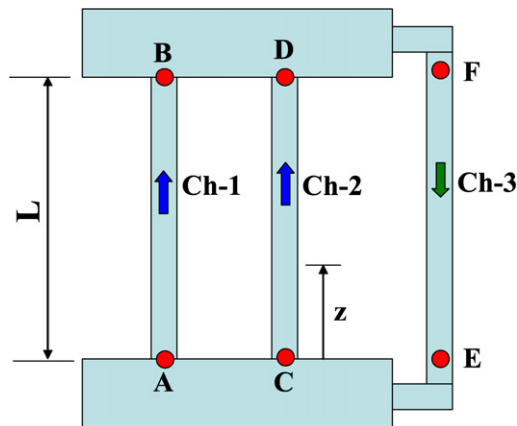
where $dz = ds \sin \theta$.

Noting that $\oint dv = 0$ and $\oint dP = 0$ for a closed loop, we can write

$$0 = -g \oint \rho dz - \frac{f W^2 L_t}{2D\rho A^2} - \frac{K W^2}{2\rho A^2} \quad (\text{A.5})$$

$$-g \oint \rho dz = \sum \left(\frac{fL}{D} + K \right) \frac{W^2}{2\rho A^2} \quad (\text{A.6})$$

Without loss of generality, the condition for possible metastable flow regime has been derived for a two parallel heated channels with a common down-comer system as follows:



Now, considering the closed loop formed by Ch-1 and Ch-3 (shown in Fig. I), Eq. (A.6) becomes

$$-g \left[\int_A^B \rho dz + \int_F^E \rho dz \right] = \sum_A^B \left(\frac{fL}{D} + K \right) \frac{W_1^2}{2\rho A^2} + \sum_F^E \left(\frac{fL}{D} + K \right) \frac{(W_1 + W_2)^2}{2\rho A^2} \quad (\text{A.7})$$

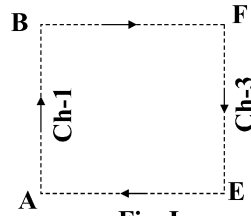


Fig. I

Now, considering the closed loop formed by Ch-2 and Ch-3 (shown in Fig. II) Eq. (A.6) becomes

$$-g \left[\int_C^D \rho dz + \int_F^E \rho dz \right] = \sum_C^D \left(\frac{fL}{D} + K \right) \frac{W_2^2}{2\rho A^2} + \sum_F^E \left(\frac{fL}{D} + K \right) \frac{(W_1 + W_2)^2}{2\rho A^2} \quad (\text{A.8})$$

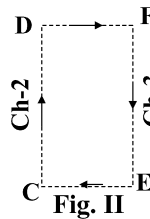


Fig. II

Since, $z_B - z_A = z_D - z_C = z_F - z_E = L$, Eqs. (A.7) and (A.8) becomes

$$(\bar{\rho}_3 - \bar{\rho}_1)gL = \sum_{\text{Ch-1}} \left(\frac{fL}{D} + K \right) \frac{W_1^2}{2\bar{\rho}_1 A^2} + \sum_{\text{Ch-3}} \left(\frac{fL}{D} + K \right) \frac{(W_1 + W_2)^2}{2\bar{\rho}_3 A^2} \quad (\text{A.9})$$

Similarly,

$$(\bar{\rho}_3 - \bar{\rho}_2)gL = \sum_{\text{Ch-2}} \left(\frac{fL}{D} + K \right) \frac{W_2^2}{2\bar{\rho}_2 A^2} + \sum_{\text{Ch-3}} \left(\frac{fL}{D} + K \right) \frac{(W_1 + W_2)^2}{2\bar{\rho}_3 A^2} \quad (\text{A.10})$$

The flow in Ch-2 to get reversed, a local loop has to be set up between Ch-1 and Ch-2. This will happen only when the buoyancy force available between Ch-1 and Ch-2 overcomes that of buoyancy force between Ch-2 and Ch-3. That is, for flow reversal from up-flow to down-flow the condition that should be satisfied is

$$(\bar{\rho}_2 - \bar{\rho}_1)gL \geq (\bar{\rho}_3 - \bar{\rho}_2)gL \quad \text{or} \quad (\bar{\rho}_2 - \bar{\rho}_1)gL \geq (\bar{\rho}_{DC} - \bar{\rho}_2)gL \quad (\text{A.11})$$

Conversely, the flow reversal criteria from down-flow to up-flow can be given as

$$(\bar{\rho}_3 - \bar{\rho}_2)gL \geq (\bar{\rho}_2 - \bar{\rho}_1)gL \quad \text{or} \quad (\bar{\rho}_{DC} - \bar{\rho}_2)gL \geq (\bar{\rho}_2 - \bar{\rho}_1)gL \quad (\text{A.12})$$

At limiting case, just before flow reversal $(\bar{\rho}_2 - \bar{\rho}_1)gL = (\bar{\rho}_3 - \bar{\rho}_2)gL$

Table A.1
Density difference among the channels before and after flow reversal using RELAP5

	$(\bar{\rho}_{DC} - \bar{\rho}_1)$ in kg m^{-3}	$(\bar{\rho}_{DC} - \bar{\rho}_2)$ in kg m^{-3}	$(\bar{\rho}_2 - \bar{\rho}_1)$ in kg m^{-3}	$(\bar{\rho}_2 - \bar{\rho}_3)$ in kg m^{-3}	Case No.
Before flow reversal	6.13	6.13	2.99–6	2.44e–6	Case-1
After flow reversal	3.70	0.26	3.43	3.29	
Before flow reversal	3.74	3.74	5.19e–4	5.19e–4	Case-2
After flow reversal	2.31	0.15	2.15	2.07	
Before flow reversal	3.73	0.27	3.44	3.29	Case-3
After flow reversal	6.16	6.16	2.23e–6	2.23e–6	
Before flow reversal	2.21	0.053	2.19	2.17	Case-4
After flow reversal	3.19	2.81	0.35	0.35	

$$\begin{aligned}
 & \sum_{\text{Ch-1}} \left(\frac{fL}{D} + K \right) \frac{W_1^2}{2\bar{\rho}_1 A^2} + \sum_{\text{Ch-2}} \left(\frac{fL}{D} + K \right) \frac{W_2^2}{2\bar{\rho}_2 A^2} \\
 &= \sum_{\text{Ch-2}} \left(\frac{fL}{D} + K \right) \frac{W_2^2}{2\bar{\rho}_2 A^2} + \sum_{\text{Ch-3}} \left(\frac{fL}{D} + K \right) \frac{(W_1 + W_2)^2}{2\bar{\rho}_3 A^2} \\
 & \sum_{\text{Ch-1}} \left(\frac{fL}{D} + K \right) \frac{W_1^2}{2\bar{\rho}_1 A^2} = \sum_{\text{Ch-3}} \left(\frac{fL}{D} + K \right) \frac{(W_1 + W_2)^2}{2\bar{\rho}_3 A^2}
 \end{aligned} \tag{A.13}$$

In case of a four parallel channel system that has been analyzed by RELAP5/MOD3.2 computer code, the down-comer is equivalent to the Ch-3 of the above mentioned derivation. In order to validate the analytical condition given in Eqs. (A.11) and (A.12), the average density difference among the channels has been calculated using RELAP5 before and after flow reversal and given in a tabular form in Table A.1.

A.2. Explanation of flow reversal from RELAP5 results

Here Case-1 corresponds to the situation when all three channels were equally heated with a heat flux of 10 kW m^{-2} and after steady state, the heat flux in Ch-2 was reduced to cause flow reversal in that channel. Before flow reversal, the average density difference between down-comer and Ch-2 (6.13 kg m^{-3}) is higher than that between Ch-2 and Ch-1 ($2.99\text{e}-6 \text{ kg m}^{-3}$) (please see Table A.1). Clearly this shows before flow reversal the loop is between Ch-2 and down-comer. Whereas after flow reversal the average density difference between Ch-2 and Ch-1 (3.43 kg m^{-3}) has overtaken that between down-comer and Ch-2 (0.26 kg m^{-3}). The average density difference between Ch-2 and Ch-3 has also risen considerably, which will in turn promote flow reversal in Ch-2 (up-flow to down-flow) as the flow in Ch-3 is upward. This is consistent with our analytical condition given in Eq. (A.11). Similar explanation can be given for Case-2 where the initial starting heat fluxes in each of the three channels were 5 kW m^{-2} .

Now, Case-3 corresponds to the situation where two channels (Ch-1 & Ch-3) were given an equal heat flux of 10 kW m^{-2} and Ch-2 remained unheated up to steady state. After steady state the heat flux in Ch-2 was raised to cause flow reversal in that channel. It can be observed in the table that the flow reversal

is taking place when the average density difference between down-comer and Ch-2 overtakes that of Ch-2 and Ch-1. This paves the way to set up a local loop between down-comer and Ch-2 as suggested in Eq. (A.12) and in conformity with our theory. Similar explanation can be given for Case-4 where the initial starting heat fluxes were 5 kW m^{-2} .

References

- [1] J.C. Chato, Natural convection flows in parallel-channel systems, *Journal of Heat Transfer* 85 (1963) 339–345.
- [2] Y. Zvirin, The onset of flows and instabilities in a thermosyphon with parallel loops, *Nuclear Engineering and Design* 92 (1986) 217–226.
- [3] T. Takeda, H. Kawamura, M. Seki, Natural circulation in parallel vertical channels with different heat inputs, *Nuclear Engineering and Design* 104 (1987) 133–143.
- [4] R. Yahalom, M. Bein, Boiling thermal hydraulic analysis of multichannel low flow, *Nuclear Engineering and Design* 53 (1979) 29–38.
- [5] N.E. Todreas, M.S. Kazimi, *Nuclear System II, Elements of Thermal Hydraulic Design*, Hemisphere, New York, 1990.
- [6] W. Linzer, H. Walter, Flow reversal in natural circulation systems, *Applied Thermal Engineering* 23 (2003) 2363–2372.
- [7] C.D. Fletcher, R.R. Schultz, RELAP5/MOD3 Code Manual Volume II: User's Guide and Input Requirements, Idaho National Engineering Laboratory, Idaho, USA, 1995.
- [8] S.K. Mousavian, M. Misale, F. D'Auria, M.A. Salehi, Transient and stability analysis in single-phase natural circulation, *Annals of Nuclear Energy* 31 (2004) 1177–1198.
- [9] M. Misale, M. Frogheri, F. D'Auria, E. Fontani, A. Garcia, Analysis of single-phase natural circulation experiments by system codes, *International Journal of Thermal Sciences* 38 (1999) 977–983.
- [10] W. Ambrosini, N. Forgone, J.C. Ferreri, M. Bucci, The effect of wall friction in single-phase natural circulation stability at the transition between laminar and turbulent flow, *Annals of Nuclear Energy* 31 (2004) 1833–1865.
- [11] M.T. Kamble, A. Chakravarty, D.S. Pilkhwal, P.K. Vijayan, D. Saha, R.K. Sinha, Simulation of single phase natural circulation in a rectangular loop using RELAP5/MOD3.2, in: 1st National Conference on Nuclear Reactor Safety, November 25–27, 2002, Mumbai, India.
- [12] P. Welander, On the oscillatory instability of a differentially heated fluid loop, *Journal of Fluid Mechanics* 29 (1) (1967) 17–30.
- [13] H.F. Creveling, J.F. De Paz, J.Y. Baladi, R.J. Schoenhals, Stability characteristics of a single-phase free convection loop, *Journal of Fluid Mechanics* 67 (1975) 65–84.
- [14] H.H. Bau, K.E. Torrance, On the stability and flow reversal of an asymmetrically heated open convection loop, *Journal of Fluid Mechanics* 106 (1981) 417–433.